Petroleum & Coal
ISSN 1337-7027

Available online at www.vurup.sk/petroleum-coal
Petroleum & Coal 57(5) 516-525, 2015

PROMOTIONAL EFFECTS OF CERIA AND CALCIUM OVER CNTS-SUPPORTED COBALT CATALYST IN FISCHER-TROPSCH SYNTHESIS

Sophia Mohamadnasab Omran[1], Ahmad Tavasoli*[i], Yahya Zamani[2]

[1]School of Chemistry, College of Science, University of Tehran, Tehran 1513746911, Iran
[2]Research Institute of Petroleum Industry (RIPI), National Iranian Oil Company, Tehran, Iran

Received August 11, 2015, Accepted November 30, 2015

Abstract

In this study, the effect of Ca and Ce and Synergetic effects of these promoters on the catalytic properties of 15wt.% Co/CNTs catalyst in Fischer-Tropsch synthesis (FTS) are investigated. Catalysts with atomic ratios of 100Co, 100Co/2Ca, 100Co/2Ce and 100Co/1Ca/1Ce were prepared. Catalysts were characterized by BET, TPR, XRD and H_2 chemisorption techniques. The FTS performance of the catalysts was studied in a fixed-bed micro-reactor under conditions of 220°C, 18bar, and H_2/CO = 2 (v/v). Addition of small amounts of Ce to the Co/CNTs catalyst shifted both TPR peaks significantly to the lower temperatures. According to XRD results, average crystallite sizes of Co decreased in Co-Ce/CNTs and Co-Ce-Ca/CNTs catalysts. In Ca promoted catalyst in comparison with unprompted catalyst, the FTS activity decreased slightly and C_5^+ selectivity increased by about 12.5%. Addition of Ce increased the FTS activity by about 10.3% and increased C_5^+ selectivity from 72% to 77%. Synergistic effects of Ca and Ce in Co-Ca-Ce/CNTs, caused significant increase of C_{5+} selectivity to 80%. Explanations for the selectivity trends are provided based on the effects of Ce, Ca on structural and electronic properties of Co/CNTs catalysts.

Keywords: Fischer–Tropsch synthesis; Cobalt; promoter; Synergetic effect.

1. Introduction

Fischer–Tropsch synthesis (FTS) is an established technological route for upgrading natural gas, coal and biomass to liquid fuels and other chemicals. In the FTS process, high molecular weight hydrocarbons are synthesized by catalytic hydrogenation of carbon monoxide [1-3]. The typical active metals used in Fischer-Tropsch catalysts are Fe, Co and Ru. Among these metals, Co-based catalysts are generally more active and more selective to liner long-chain hydrocarbons [4-5]. In order to achieve high surface active sites (Co^o), cobalt precursors are dispersed on porous carriers such as oxides (SiO_2, Al_2O_3, TiO_2) and carbon-based supports [6-12]. Using carbon nanotubes as cobalt catalyst support was found to cause the reduction temperature of cobalt species to shift to lower temperatures. The strong metal-support interaction are reduced to a large extend and the reducibility of the catalysts improved significantly [12-16].

These catalysts are often loaded with small amounts of promoter elements that enhance their overall catalytic performances and lifetime [17]. It is generally accepted that promoter elements may induce these beneficial effects in several manners. The family of promoter elements divided into two classes according to their intended function. Structural promoters affect the formation and stability of the active phase of a catalyst material, whereas electronic promoters directly affect the elementary steps involved in each turnover on the catalyst [18]. Co-based catalysts generally require promoters such as alkali metal ions, noble metals, or transition metal oxides to attain optimum catalytic performance [12]. It is believed that alkali addition to cobalt catalysts supported on SiO_2, Al_2O_3 and TiO_2 leads to an enhanced adsorption of carbon monoxide and that the growth probability of Fischer-Tropsch synthesis increases

up to α = 0.87 in the presence of alkali promoters. For the cobalt catalysts supported on SiO_2 and Al_2O_3, it has been shown that, addition of small amounts of calcium oxide as a promoter improves the cobalt oxide reducibility and reduces the formation of cobalt-aluminate and cobalt-silicate species. A positive correlation between basicity and particle size was observed. The addition of calcium to the cobalt catalysts supported on Al_2O_3 was found to greatly maintain selectivity to C_5^+ for a wide range of H_2/Co molar ratios [19-20]. Many transition metal oxides and rare earth oxides such as, ZrO_2, MnOx, La_2O_3 and CeO_2 have been investigated as potential promoters for Co-based FTS catalysts supported on SiO_2, Al_2O_3 and TiO_2 [21]. These optimized ceria-promoted catalysts exhibit good activity, C_5^+ selectivity and stability. It is suggested that ceria could enhance the dispersion of metallic cobalt and increase the amount of active sites for FTS, leading to increase concentration of surface active carbon species and selectivity towards long chain hydrocarbons [22].

The aim of the present work is to study the effect of Ca and Ce oxides on the performance of carbon nanotubes supported cobalt FTS catalysts and to investigate the synergetic effects of Ce and Ca promoters on the FTS activity and product distribution, using a bench scale experimental device.

2. Experimental

2.1 Catalyst preparation

Nanostructure 15 wt.% Co/CNTs catalysts promoted with Ca, Ce, Ca-Ce and unpromoted 15 wt.% Co/CNTs catalysts were prepared by incipient wetness impregnation method. First, CNTs were impregnated with aqueous solutions of cobalt nitrate [$Co(NO_3)_2.6H_2O$] as active metal, calcium nitrate [$Ca(NO_3)_2.4H_2O$] and cerium nitrate [$Ce(NO_3)_2.6H_2O$] as promoters. After impregnation, the catalysts were dried at 120 °C for 2 h and then calcined at 350°C for 4 h. The catalyst compositions were designated in terms of atomic ratios as 100Co, 100Co/2Ca, 100Co/2Ce and 100Co/1Ca/1Ce.

2.2 Catalyst characterization

2.2.1 BET surface area measurements

The surface area, pore volume, and average pore radius of the catalysts were measured by a Micromeritics ASAP-3020 system. The samples were degassed at 300°C for 2 h under 50 mTorr vacuum and their BET area, pore volume, and average pore radius were determined.

2.2.2 X-ray diffraction

XRD measurements of the calcined catalysts were conducted with a Philips PW1840 X-ray diffractometer with monochromatized Cu/Ka radiation. The average size of the Co_3O_4 crystallites in the calcined catalysts was estimated from the line broadening of a Co_3O_4 at 2θ of 36.8° using Scherrer equation:

$$d = \frac{k\lambda}{\beta(\theta)Cos\theta} \quad (1)$$

where λ is the X-ray wavelength (nm), $\beta(\theta)$is the full width at half maximum (rad) of the identification peak, $\theta$is the diffraction angle and $K$is a constant typical of the equipment.

2.2.3. Temperature-programmed reduction (TPR)

Temperature programmed reduction (TPR) spectra of the calcined catalysts were recorded using a Micromeritics TPD-TPR 290 system, equipped with a thermal conductivity detector. The catalyst samples were first purged in a flow of argon at 400°C, to remove traces of water vapor and other adsorbents, and then cooled to 40°C. The TPR of 50 mg of each sample was performed using 5% hydrogen in argon gas mixture with a flow rate of 40 cm^3/min. The samples were heated from 50 to 900°C with a linear heating rate of 10°C/min.

2.2.4 Hydrogen chemisorption and reoxidation

The amount of chemisorbed hydrogen on the catalysts was measured using the Micromeritics TPD-TPR 290 system. 0.25 g of the sample was reduced under hydrogen flow at 400°C for 12 h and then cooled to 100°C under hydrogen flow. Then, the flow of hydrogen was switched to argon at the same temperature, which lasted about 30 min in order to remove the weakly adsorbed hydrogen. Afterwards, the temperature-programmed desorption (TPD) of H_2 over the samples was obtained by increasing the temperature of the samples, with a ramp rate of 10°C/min, to 400°C under the argon flow. H_2-TPD measurement was used to determine the cobalt dispersion and its surface average crystallite size. After H_2-TPD, the sample was reoxidized at 400°C by pulses of 10% oxygen in helium to determine the extent of catalyst reduction. It is noted that during reoxidation of the catalysts no CO_2 peak is observed indicating that CNT as support of the catalyst has not reacted with oxygen in the oxygen titration test. It is assumed that Co^o is oxidized to Co_3O_4. The calculations are summarized as follows.

$$\%Dispersion = \frac{number\ of\ Co^0 atoms\ on\ surface}{number\ of\ Co\ atoms\ in\ sample} \times 100 \quad (2)$$

$$Fraction\ reduced = \frac{O_2\ Uptake \times \frac{2}{3} \times atomic\ weight}{Percentage\ metal} \quad (3)$$

2.2.5 Cata-test system and pretreatment procedures

The catalysts were evaluated in terms of their FTS activity (gCH/(g cat·h)) and selectivity (the percentage of the converted CO that appears as hydrocarbon products) in a fixed bed down-flow micro-reactor. The reactor temperature was controlled via a PID temperature controller. Brooks 5850 mass flow controllers were used to add H_2 and CO at desired flow rates into the reactor. Prior to the activity tests, the catalysts activation was conducted according to the following procedure. 1.5 g catalyst was placed in the reactor and pure hydrogen was introduced at a flow rate of 60 mL/min. The reactor was heated from room temperature to 400°C with a heating rate of 2°C/min. It was maintained at the activation condition for 20 h and the catalyst was reduced and activated in situ. After the reduction and activation period, the reactor temperature was cooled down to 180°C under flowing hydrogen. The mixed gases entered from top of the reactor. Synthesis gas (H_2/CO moral ratio of 2) was introduced and the reactor pressure was increased to 1.8 MPa. The reactor temperature was then increased to 220°C at a rate of 2°C/min. Synthesis were carried out for a period of 14 days. Products were continuously removed from the reactor and passed through two traps, one maintained at 100°C (hot trap) and the other at 0°C (cold trap). The uncondensed vapor stream was reduced to atmospheric pressure through a back pressure regulator. The outlet flow was measured with a bubble-meter and its composition quantified using an on-line Varian 3800 gas chromatograph. The contents of hot and cold traps were removed every 12 h, the hydrocarbon and water fractions separated, and then analyzed by GC. CO conversion and different product selectivities (the percentage of the converted CO that appears as a given product) were calculated based on the GC analyses.

3. Results and discussion

3.1 Textural property analysis

The surface area and pore size distribution of the fresh catalysts are shown in Table 1. BET surface area, pore volume of the CNTs were 226.6(m^2/g) and 0.79(cm^3/g). It was clear that BET surface area and pore volume of the catalysts decreased in different extend, indicating that cobalt oxides and promoters oxides partly entered the pores of the support and partly dispersed on the surface of the support and jammed some pore path [23- 25]. The catalyst promoted with Ca had the lowest BET surface area and pore volume that indicates some more pores blockage due to promoting cobalt with Ca loading on the support.

Table 1 The composition and textural properties of the catalysts

Catalyst	Catalyst composition	BET surface area (m^2/g)	Pore volume (cm^3/g)	Average pore size (nm)
Co/CNTs	100Co	209	0.57	110
Co-Ca/CNTs	100Co/2Ca	193	0.49	98
Co-Ce/CNTs	100Co/2Ce	198	0.52	106
Co-Ca-Ce/CNTs	100Co/1Ca/1Ce	196	0.50	104

3.2 XRD measurements

Figure1 shows the XRD patterns of the calcined fresh catalysts. The diffraction peaks of Co_3O_4 appeared in all XRD patterns of the catalysts, suggesting that the cobalt oxides were dispersed on the CNTs [26- 28].

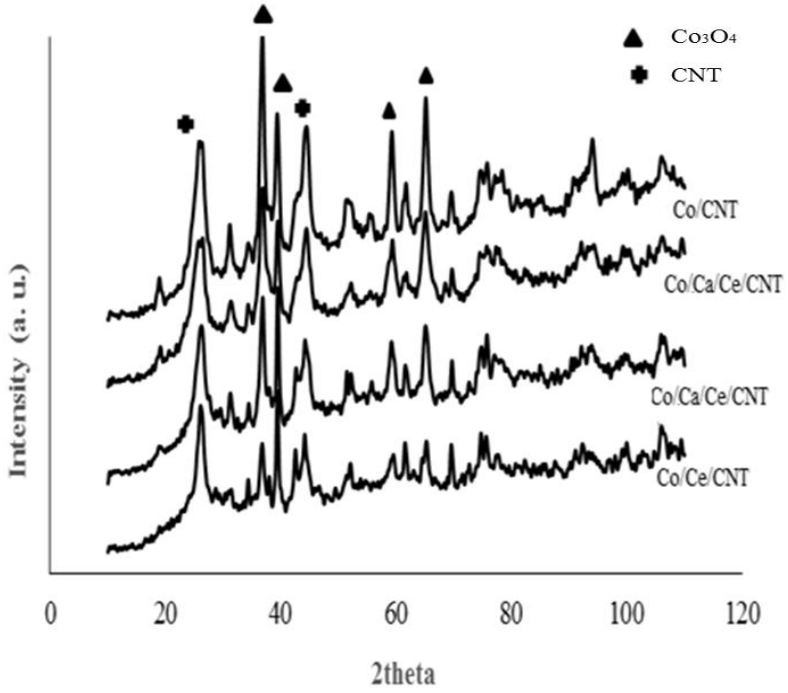

Figure 1 XRD spectra of the fresh catalysts

The cobalt oxide phases for the fresh catalysts determined by fitting the XRD patterns. Peaks at 2Θ values of 25 and 43° corresponded to CNTs support while the other peaks related to the different crystal planes of Co_3O_4. In the case of Co-Ce/CNT catalyst, the intensity of Co_3O_4 addition peak declined, indicating that the crystallite size of Co_3O_4 decreased and its dispersion increased. Increasing the dispersion and reducing the active metal particle sizes during catalyst pretreatment step will in increase the reduced surface metallic cobalt, which are the key active components for FT reaction. In the XRD pattern of the catalysts promoted with Ca and Ce, there was no diffraction peak for Ca and Ce oxides. The reason was that promoters had low content and indicating that alkali-earth oxides were dispersed on the support as a monolayer or formed spinel-like or tridymite-like structure with no detectable interaction between the promoters and support [29,19].The average particle size for the catalysts was calculated from the XRD patterns and Scherrer formula. Based on XRD patterns, the average particle sizes for the Co/CNTs, Co-Ca/CNTs, Co-Ce/CNTs and Co-Ca-Ce/CNTs catalysts are 9.8, 10.1, 7.9, and 8.4 nm, respectively.

3.3 TPR measurements

The reduction behavior of the various catalysts was studied by temperature-programmed reduction (TPR). It has been shown that, pure Co_3O_4 has two reductive peaks at 347 °C and 438°C, corresponding to the reduction of Co_3O_4 to CoO and CoO to Co, respectively [30]. The TPR spectra of the calcined Co/CNTs, Co-Ca/CNTs, Co-Ce/CNTs and Co-Ca-Ce/CNTs catalysts are shown in figure 2. This figure shows that addition of small amounts of Ce to the cobalt catalyst shifts both TPR peaks significantly to the lower temperatures. Also, for Co-Ce/CNTs and Co-Ca-Ce/CNTs catalysts significant improvement in the reducibility of the catalyst is observed. The reduction of cerium oxide occurs at temperatures lower than that of the cobalt, so it can be concluded that reduced Ce enhances the reduction of cobalt oxides, by spillover of hydrogen from Ce to the cobalt oxides [31]. The TPR profiles of calcium promoted catalyst indicate that addition of calcium to the Co catalyst slightly increases the temperature of the first and the second TPR peaks, suggesting difficult reduction process for small cobalt species due to higher interaction with support. Comparing the data show that ceria and ceria + calcium promoted cobalt catalysts are reduced more easily than those promoted with calcium.

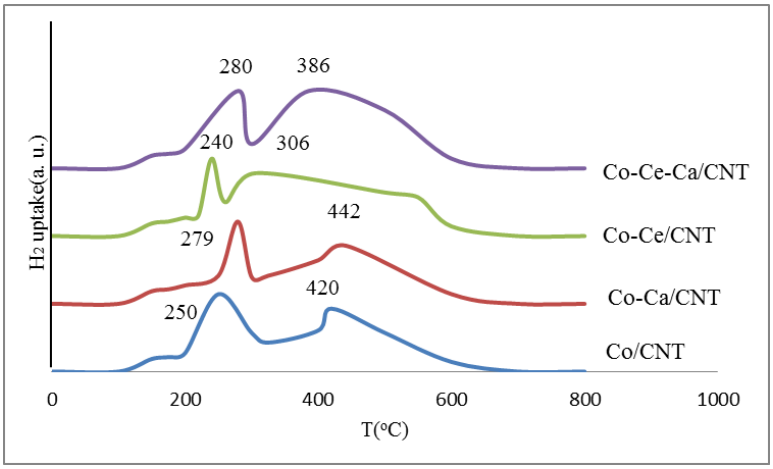

Figure 2 TPR curves for all the catalysts

3.4 Hydrogen chemisorption and reoxidation

Percentage dispersion and sizes of the cobalt particles determined by H_2-TPD and pulse reoxidation of the calcined catalysts are given in Table 2. For each sample, dispersion and particle size were calculated based on the total amount of cobalt in the catalyst samples. The percentage of reduction was measured from the oxygen titration after H_2-TPD, assuming Co^o is reoxidized to Co_3O_4. Comparing the results of TPD and oxygen titrations of the calcined Co/CNTs, Co-Ca/CNTs, Co-Ce/CNTs and Co-Ca-Ce/CNTs nano catalysts in Table 2, it is clear that the hydrogen uptake increases significantly using Ce as cobalt catalyst promoter.

Table 2. %Dispersion and crystallite sizes of cobalt particles determined by H_2 TPD and pulse reoxidation of calcined catalysts.

Catalyst	μ mole H2 desorbed /g cat.	μ mole O_2 Consumed /g cat.	%Red.	%Dispersion	dp (nm)
Co/CNT	198	1223	64	19.5	9.5
Co-Ca/CNT	187	1087	56.8	18.4	10
Co-Ce/CNT	242	1382	72.3	23.8	7.8
Co-Ca-Ce/CNT	212	1271	66.6	21.8	8.5

In agreement with the results of TPR, results in Table 2 indicate that a remarkable improvement in the percentage reduction is obtained by addition of Ce to CNTs supported cobalt catalyst. While the dispersion of the cobalt crystallites calculated based on the total amount of cobalt increases significantly, the average cobalt particle size decreases, which is due to lower degree of agglomeration of the cobalt crystallites in Co-Ce/CNTs and Co-Ca-Ce/CNTs catalysts. These results are in agreement with the results of XRD and tests. Higher dispersion and lower cobalt cluster size will increase the number of sites available for FT reaction in the Ce promoted catalysts in comparison with the unpromoted and Ca promoted catalysts.

3.5 FTS performances

FTS performances of the catalysts were measured in a fixed-bed reactor under conditions of 220°C, 18 bar, and H_2/CO = 2 (v/v). Gas, water, light and heavy hydrocarbon samples were collected and analyzed. A heavy wax sample was taken from the hot trap. Vapor phase passed the hot and clod traps outside the reactor. The wax was collected from the hot trap and an oil plus water sample from the cold trap. Tail gas from the cold trap was analyzed with GC. Carbon monoxide conversion was calculated based on the gas product GC analysis results and the gas flow measured at the reactor outlet. Carbon monoxide and syngas conversion were obtained using the following formula:

$$\text{Conversion} = \frac{N_{\text{in}} - N_{\text{out}}}{N_{\text{in}}} \times 100\% \qquad (4)$$

3.5.1 Carbon monoxide conversion

In the FTS process, the conversion of syngas over a catalyst is one of the most pivotal steps. The activities and product selectivities were tested over a period of 14 day runs. Figure 3 presents the results of CO conversion with time on stream. Comparing results of the first day reveals that by addition of Ce as promoter CO conversion shows a remarkable increase. CO conversion increased from 78% in the case of unpromoted cobalt catalyst to 86% and 85% for Co-Ce/CNTs and Co-Ce-Ca/CNTs catalysts, respectively.

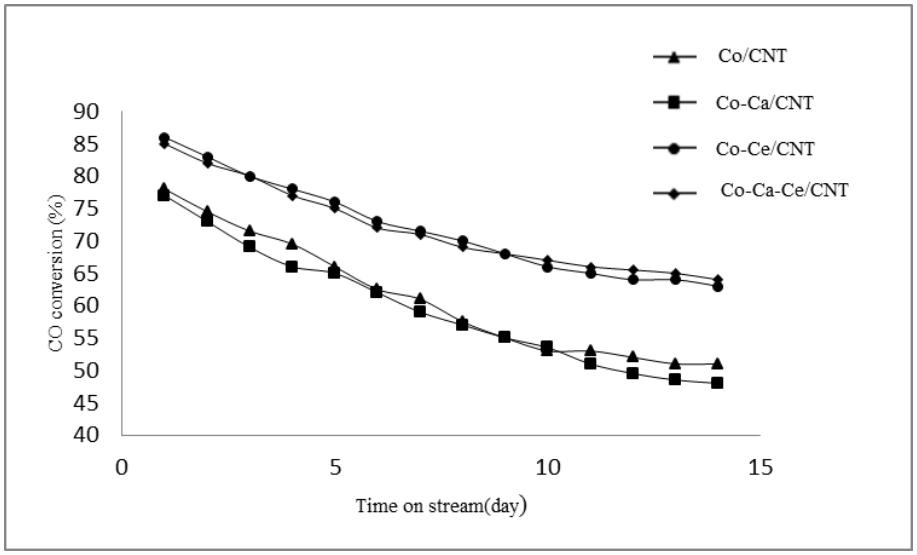

Fig. 3 Co conversion (%) variation with time on stream (T = 220°C, P = 1.8 MPa, H2/CO = 2)

This figure shows that promotion of cobalt catalyst with Ca decreased the CO conversion to 77%. The average of the CO conversion for Co-Ce/CNTs and Co-Ca/CNTs catalysts is equal to 81.5%. This shows that the catalyst with double promotions of Ca and Ce significantly improved the FTS activities, higher than the average of catalyst with single promotion of Ca and Ce, which are due to the synergistic effect. The changes in catalyst performance during

FT synthesis can be a result of geometric effects. The main function of structural promoters is to influence the cobalt dispersion by governing the cobalt-support oxide interaction [32]. A high Co dispersion results in a high active Co metal surface and, therefore, in a high coverage by the reactants, and as a consequence an improved catalyst activity. These results observed in the present work for catalysts with Ce and Ce+Ca promoters. Figure 3 also shows that, for all catalysts the CO conversion sharply decreases in the first days, and then levels off. The trend of CO conversion decline and the amount of CO conversion drop are similar for all the catalysts. This indicates that the promoters do not change the catalyst stability. However, catalyst stability is an important performance variable in cobalt catalyzed FT processes, and should be studied carefully.

3.5.2 Product selectivity

Figures 4 and 5 present the CH_4 and C_5^+ selectivities for all the catalysts during the first 24 h FT synthesis. As shown, addition of ceria causes only small changes on the CH_4 and C_5^+selectivities, but calcium causes significant increase in C_5^+ selectivity and decreases the generation rate of methane to a large extent. This figure also shows that the catalyst with double promotions of Ca and Ce increases the C_5^+selectivity to 80% , which is higher than the average of the catalysts with single promotion of Ca and Ce. This can be due to the synergistic effects of Ca and Ce. Alkalis such as Ca can cover active Co sites and discourage H_2 dissociation. H_2 generally requires two adjacent metal sites to dissociate [33-35]. A decrease in available surface H reduces CH_4 selectivity and increases selectivity to larger hydrocarbon products [36-38].

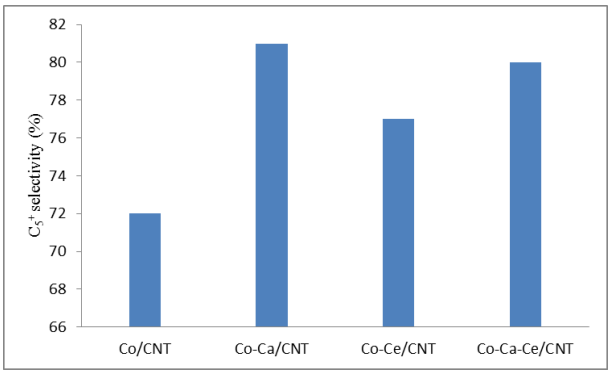

Fig.4 Variation of C_{5+} selectivity for all the catalyst

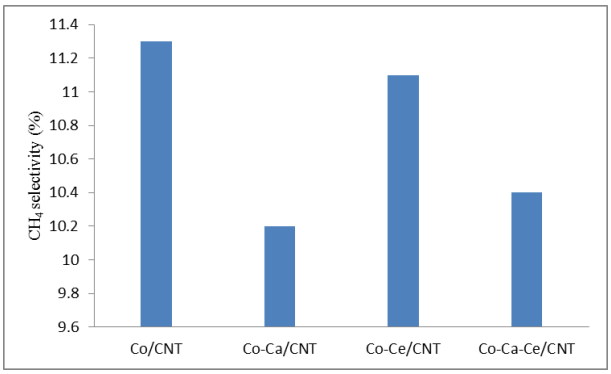

Fig. 5 Variation of CH_4 selectivity for all the catalyst

Comparing the results on sections 3.5.1 and 3.5.2 shows that, addition Ca to Co/CNTs catalyst increases the C_5^+ selectivity but Ca has a negligible effect on Co dispersion and slightly hindered catalyst reducibility by increasing the Co reduction temperatures. Ca was found to decrease catalyst activity and selectivity to CH_4, while increased selectivity to C_5^+ hydrocarbons. These effects are attributed minimally to geometric effects of surface alkalis, which can block active catalyst sites, and mostly to electronic effects which have been shown to affect H_2 and CO adsorption and dissociation. Addition Ce to Co/CNTs catalyst increased CO conversion. Ce improved catalyst reducibility, and decreased the Co reduction temperatures. This might be due to the migration of adsorbed hydrogen to the bulk, or the spillover of hydrogen from cobalt to ceria. For the catalyst with double promotions of Ca and Ce, structural effects of Ce and electronic effects of Ca worked together and synergistic effects of Ca and Ce significantly increased C_5^+ selectivity to 80% and CO conversion to 85%.

Figure 6 shows the selectivity variations of methane and C_5^+ liquid hydrocarbon with reaction time. Figure 6 displays that for all catalysts, the selectivity of CH_4 decreases with time-on stream during 14 days FT synthesis. Also, Figure 6 shows that for all catalysts the C_5^+ selectivity increases during 14 days FT synthesis. It has been shown that the larger cobalt particles are more selective to higher molecular weight hydrocarbons and smaller cobalt particles are

selective to methane and light gaseous hydrocarbons [39]. Sintering of smaller Co particles during FT synthesis and formation of larger Co particles leads to enhancement of C_5^+ selectivity and suppression of CH_4 production with time on stream.

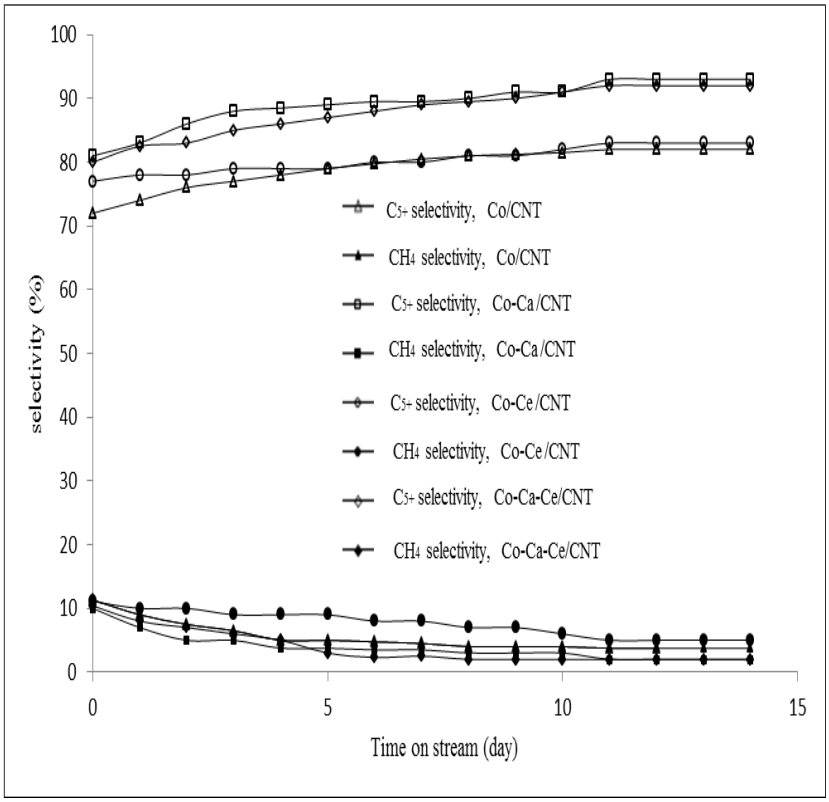

Figure 6. Liquid C_{5+} hydrocarbon selectivity variation with time on stream (T = 220°C, P = 1.8 MPa, H2/CO = 2)

4. Conclusions

Promotion of nano-sized cobalt catalyst with Ca and Ce was found to have significant effects on the adsorption, dispersion and reduction behaviors of cobalt catalysts as well as their catalytic performances during Fischer–Tropsch synthesis (FTS). Addition Ca to Co/CNTs catalyst increased C_5^+ selectivity to 81%. Ca was found to decrease catalyst activity and selectivity to CH_4, while increased selectivity to C_5^+ hydrocarbons. Addition Ce to Co/CNTs catalyst increased CO conversion to 86%. For the catalyst with double promotions of Ca and Ce, structural effect of Ce and electronic effect of Ca worked together and synergistic effects of Ca and Ce significantly increased C_5^+ selectivity to 80% and %CO conversion to 85%.

References

[1] Wang T, Wang J, Jin Y. Slurry Reactors for Gas-to-Liquid Processes. Industrial & Engineering chemistry research 2007; 46: 5847-5824.

[2] Zhang CH, Yang Y, Teng BT, Li TZ, Zheng HY, Xiang HW, Li YW. Study of an iron-manganese Fischer-Tropsch synthesis catalyst promoted with copper. Journal of catalysis 2006;237: 415-405.

[3] Kang SH, Woo KJ, Jun KW, Kang Y. Hydrogenation of CO on supported cobalt γ-Al2O3 catalyst in fixed bed and slurry bubble column reactors, Korean Journal of Chemical Engineering 2009;26: 1538-1533.

[4] Iglesia. E. Design, synthesis, and use of cobalt-based Fischer-Tropsch synthesis catalysts. Applied Catalysis A 1997;161:78–59.

[5] Khodakov AY, Chu W, Fongarland P. Advances in the development of novel cobalt Fischer-Tropsch catalysts for synthesis of long-chain hydrocarbons and clean fuels. Chemical reviews 2007;107:1744–1692.
[6] Dry ME, Anderson JR, Boudart M. The Fischer-Tropsch synthesis Catalysis. Science and Technology 1981;1:255–159.
[7] Bartholomew CH, New Trends in CO Activation. L. Guczi (Ed.). Amsterdam; 1991.
[8] Jung HJ, Walker PL, Vannice M A. CO Hydrogenation over Well-Dispersed Carbon-Supported Iron Catalysts. Journal of Catalysis 1982;75:422–416.
[9] Jung, M. A. Vannice, L. N. Mulay, R. M. Stanfield, W. N. Delgass. SMSI effects *on* CO adsorption and hydrogenation *on* Pt catalysts. Journal of Catalysis 1982;76:224–208.
[10] Venter J, Kaminsky M, Geoffroy M, Vannice M A. Carbon-supported Fe-Mn and K-Fe-Mn clusters for the synthesis of C2-C4 olefins from CO and H2**:** I. Chemisorption and catalytic behavior. Journal of Catalysis 1987;130:465–450.
[11] Venter J, Kaminsky M, Geoffroy M, Vannice M A. Carbon-supported Fe-Mn and K-Fe-Mn clusters for the synthesis of C2-C4 olefins from CO and H2 : II. Chemisorption and catalytic behavior Journal of Catalysis 1987;105:162–155.
[12] Venter J, Kaminsky M, Geoffroy M, Vannice M A. The genesis of carbon-supported Fe-Mn and K-Fe-Mn catalysts from stoichiometric metal carbonyl clusters: III. Characterization by chemisorption, calorimetry, and kinetic analysis Journal of Catalysis 1989;119:466–451.
[13] Trepanier M, Tavasoli A, Dalai AK, Abatzoglou N. Co, Ru and K loadings effects on the activity and selectivity of carbon nanotubes supported cobalt catalyst in Fischer-Tropsch synthesis. Applied Catalysis A 2009;193: 362-353
[14] Guettel R, Kunz U, Turek T. Reactors for Fischer-Tropsch Synthesis Reactors for Fischer Tropsch Synthesis. Chemical Engineering & Technology 2008;31:754–746.
[15] Rofer-DePoorter CK. A Comprehensive Mechanism For the Fischer-Tropsch Synthesis, Chemical Reviews 1981;81:474–447.
[16] Bell AT. Catalytic Synthesis of Hydrocarbons over Group VIII Metals. A Discussion of the Reaction Mechanism. Catalysis Reviews Science and Engineering 1981;23: 232-203.
[17] Maitlis PM, Quyoum R, Long HC, Turner ML. Towards a chemical understanding of the Fischer-Tropsch reaction: alkene formation. Applied Catalysis A 1999;186: 374-363.
[18] Borodko Y, Somorjai GA. Catalytic hydrogenation of carbon oxides Applied Catalysis A 1999;186: 362-355.
[19] de la Osa AR, de Lucas A, Romero A, Valverde JL, Sánchez P. Co/alumina catalysts: Effect of reaction conditions. Fuel 2011;90: 1945-1935.
[20] Atashi H, Mansouri M, Hosseini SH, Khorram M, Mirzaei AA, Karimi M, Mansouri G. Intrinsic kinetics of the Fischer-Tropsch synthesis over an impregnated cobalt-potassium catalyst. Korean Journal of Chemical Engineering 2012;29: 309-304.
[21] Zhang Q, Kang J, Wang Y. Development of Novel Catalysts for Fischer–Tropsch Synthesis: Tuning the Product Selectivity. ChemCatChem 2010;2:1058-1030.
[22] Xiaoping D, Changchun Y, Ranjia L, Haibo S, Shikong S, Role of CeO2 promoter in Co/SiO2 catalyst for Fischer-Tropsch synthesis. Chinese Journal of Catalysis 2006;27:910-904.
[23] Ohtsuka Y, Arai T, Takasaki S, Tsubouchi N. Fischer-Tropsch synthesis with cobalt catalysts supported on mesoporous silica for efficient production of diesel fuel fraction. Energy and Fuels 2003,17 (4): 804-809.
[24] Jacobs G, Das TK, Zhang YQ, Li JL, Racoillet G, Davis BH. Fischer-Tropsch synthesis: support, loading and promoters on the reducibility of cobalt catalyst Applied Catalysis A 2002;233; 281-263.

[25] Zeng S, Du Y , Su H, Zhang Y. Promotion effect of single or mixed rare earths on cobalt-based catalysts for Fischer–Tropsch synthesis. Catalysis Communications 2011;13:9-6.
[26] Burakorn T, Panpranot J, Mekasuwandumrong O, Chaisuk C, Praserthdam P, Jongsomjit B.Charaterization of cobalt dispersed on the mixed nanoscale alumina and zirconia supports. Journal of Materials Processing Technology Articles 2008; 206:368-352.
[27] Girardon JS, Constant-Griboval A, Gengembre L, Chernavskii PA, Khodakov AY. Optimization of the pretreatment procedure in the design of cobalt silica supported Fischer–Tropsch catalysts. Catalysis Today 2005;106:165-161.
[28] Zhang JL, Chen JG, Ren J, Sun YH. Chemical Treatment of γ-Al2O3 and Its Influence on the Properties of Co-Based Catalysts for Fischer-Tropsch Synthesis, Applied Catalysis A 2003;243: 133-121.
[29] Horiuchi T, Hidaka H, Fukui T, Kubo Y, Horio M, Suzuki K, Mori T. Effect of added basic metal oxides on CO2 adsorption on alumina at elevated temperatures. Applied Catalysis A 1998;167:202-195.
[30] Tavasoli A, Malek Abbaslou R, Trepanier M, Dalai AK. Fischer-Tropsch synthesis over cobalt catalyst supported on carbon nanotubes in a slurry reactor. Applied Catalysis A 2008; 345:134-142.
[31] Elena Yu. KONYSHEVA. Reduction of CeO2 in composites with transition metal complex oxides under hydrogen containing atmosphere and its correlation with catalytic activity. Chemical Engineering Science 2013; 7:261-249.
[32] B. Cornils, W. A. Herrmann, R. Schlogl and C.H. Wong. Homogeneous Catalysis with Transition Metal CatalystsCatalysis from A to Z, A concise encyclopedia, Wiley-VCH, Weinheim, 2000.
[33] Zhou XL, White JM. Stabilization by potassium of adsorbed hydrogen on Pt(111). Surface Science 1987;185 (3):450-456.
[34] Solymosi F, Kovacs I. Effects of potassium adlayer on the adsorption and desorption of hydrogen on a palladium(100) surface. Journal of Physical Chemistry 1989;93. 7539 -7537.
[35] Balonek CM, Lilleb AH, Rane S, Rytter E, Schmidt LD, Holmen A. Effect of alkali Impurities metal on Co–Re Catalysts forsynthesis from biomass-derived syngas. Catalysis Letters 2010; 138 13–8.
[36] W. P. Ma, Y. J. Ding and L.W. Lin, Fischer−Tropsch Synthesis over Activated-Carbon - Supported Cobalt Catalysts: Effect of Co Loading and Promoters on Catalyst PerformanceInd. Industrial & Engineering Chemistry Research 2004;43: 2398–2391.
[37] Bonzel HP, Krebs HJ. Enhanced rate of carbon deposition during Fischer-Tropsch synthesis on K promoted Fe. Surface Science 1981;109: 527-531.
[38] Rodríguez-Ramos I, Guerrero-Ruiz A, Fierro JLG, Ramirez de la Piscina P, Homs N CO hydrogenation over potassium promoted iron, cobalt, and nickel Catalysts Prepared from Cyanide Complexes. chemical science 1990;582:211-197.
[39] Tavasoli A, Sadaghiani K, Nakhaeipour A, Ahangari M. Cobalt Loading Effects on the Structure and Activity for Fischer-Tropsch and Water-Gas Shift Reactions of Co/Al_2O_3 Catalysts. Iranian Journal of. Chemistry and Chemical Engineering 2007; 26:16-9.

[i] *Corresponding author: Ahmad Tavasoli, Tel. & Fax : +98 21 66495291, E-mail address: tavassolia@khayam.ut.ac.ir*